Regular Article

blood

TRANSPLANTATION

DR3 signaling modulates the function of Foxp3$^+$ regulatory T cells and the severity of acute graft-versus-host disease

Hidekazu Nishikii,[1,2,*] Byung-Su Kim,[1,*] Yasuhisa Yokoyama,[2] Yan Chen,[1,3] Jeanette Baker,[1] Antonio Pierini,[1] Maite Alvarez,[1] Melissa Mavers,[4] Kristina Maas-Bauer,[1] Yuqiong Pan,[1] Shigeru Chiba,[2] and Robert S. Negrin[1]

[1]Division of Blood and Marrow Transplantation, Stanford University, Stanford, CA; [2]Department of Hematology, Faculty of Medicine, University of Tsukuba, Tsukuba, Japan; [3]Department of Hematology, Central South University Xiangya Hospital, Changsha, China; and [4]Divisions of Hematology/Oncology and Stem Cell Transplantation and Regenerative Medicine, Department of Pediatrics, Stanford University, Stanford, CA

Key Points

- After DR3 activation, CD4$^+$ Foxp3$^+$ regulatory T cells showed a distinct immune phenotype and function in acute GVHD.
- Prophylactic treatment with agonistic DR3 antibody to recipient mice abrogated the lethal acute GVHD in a time-dependent manner.

CD4$^+$Foxp3$^+$ regulatory T cells (Treg) are a subpopulation of T cells, which regulate the immune system and enhance immune tolerance after transplantation. Donor-derived Treg prevent the development of lethal acute graft-versus-host disease (GVHD) in murine models of allogeneic hematopoietic stem cell transplantation. We recently demonstrated that a single treatment of the agonistic antibody to DR3 (death receptor 3, αDR3) to donor mice resulted in the expansion of donor-derived Treg and prevented acute GVHD, although the precise role of DR3 signaling in GVHD has not been elucidated. In this study, we comprehensively analyzed the immunophenotype of Treg after DR3 signal activation, demonstrating that DR3-activated Treg (DR3-Treg) had an activated/mature phenotype. Furthermore, the CD25$^+$Foxp3$^+$ subpopulation in DR3-Treg showed stronger suppressive effects in vivo. Prophylactic treatment of αDR3 to recipient mice expanded recipient-derived Treg and reduced the severity of GVHD, whereas DR3 activation in mice with ongoing GVHD further promoted donor T-cell activation/proliferation. These data suggest that the function of DR3 signaling was highly dependent on the activation status of the T cells. In conclusion, our data demonstrated that DR3 signaling affects the function of Treg and T-cell activation after alloantigen exposure in a time-dependent manner. These observations provide important information for future clinical testing using human DR3 signal modulation and highlight the critical effect of the state of T-cell activation on clinical outcomes after activation of DR3. (*Blood*. 2016;128(24):2846-2858)

Introduction

Tumor necrosis factor (TNF) family members play an important role in immune reactions through modification of T-cell activation. TNF receptor superfamily members such as CD27, CD30, OX40, HVEM, GITR, and 4-1BB are expressed on T cells, and their signaling cooperates with T-cell receptor (TCR) signaling.[1] Death receptor 3 (DR3), also known as TNF receptor superfamily 25, APO-3, TRAMP, or LARD, is a member of TNF receptor superfamily and most homologous to TNFR1.[2] DR3 binding mediates NF-kb, MAP kinase, and caspase signaling to regulate cell proliferation, activation, and differentiation in immune cells.[3,4] TL1a (TNF-like ligand 1A) is the natural ligand for DR3 and is expressed on the surface of endothelial cells, synovial fibroblasts, antigen-presenting cells, and activated T cells.[5] DR3 signaling is thought to be related to T helper 1 and T helper 17 differentiation and could be a therapeutic target for T-cell-mediated autoimmune and allergic diseases.

Conversely, DR3 signaling also plays a role in the differentiation of CD4$^+$Foxp3$^+$ regulatory T cells (Treg), which regulate the immune system and enhance immune tolerance after transplantation.[6] Analysis of DR3-deficient mice showed that DR3 signaling is required for negative selection in the thymus during T-cell development, including Treg.[7,8] In TL1a transgenic mice, Treg appear to be activated and proliferate in secondary lymphoid organs.[9] Furthermore, the administration of agonistic monoclonal antibodies to DR3 (αDR3) is reported to significantly expand Treg in a manner dependent on TCR and interleukin 2 signaling and the expanded Treg inhibited asthmatic lung inflammation in vivo.[10]

We previously demonstrated that a single injection of αDR3 could significantly expand CD4$^+$Foxp3$^+$ Treg and that T cells from αDR3-treated donor mice abrogated acute murine acute graft-versus-host disease (GVHD) without reducing GVT (graft-versus-tumor) effects.[11] However, the function of Treg after DR3 signal activation was not fully elucidated. Furthermore, the role of DR3 signaling could affect the pathophysiology of GVHD, considering the previous literature about its indispensable role in various immune reactions.[5,12] In this study, we analyzed the immune phenotype, gene expression profile, and function of DR3-activated Treg (DR3-Treg) in a murine model of allogeneic

Submitted 30 June 2016; accepted 29 September 2016. Prepublished online as *Blood* First Edition paper, 19 October 2016; DOI 10.1182/blood-2016-06-723783.

*H.N. and B.-S.K. contributed equally to this study.

The online version of this article contains a data supplement.

The publication costs of this article were defrayed in part by page charge payment. Therefore, and solely to indicate this fact, this article is hereby marked "advertisement" in accordance with 18 USC section 1734.

hematopoietic cell transplantation (HCT). We also investigated whether DR3 activation in recipient mice affects the severity of GVHD. Our data demonstrate that DR3 signaling modifies the function of Treg, but also modulates the activation status of donor T cells and the severity of acute GVHD in a time-dependent manner. Understanding these paradoxical effects of DR3 signaling in GVHD enhances our insights into the pathophysiology of GVHD and is critical for translating these concepts to the clinic.

Materials and methods

Mice and cell line

C57BL/6 (B6, H-2k^b CD45.2$^+$) and Balb/c (H-2k^d CD45.2$^+$) mice were purchased from the Jackson Laboratory (Sacramento, CA). *Luc*$^+$ C57BL/6 (B6-*luc*, H-2k^b Thy-1.1$^+$ CD45.1$^+$) and Thy-1.1$^+$ CD45.1$^+$ *gfp*$^+$ C57BL/6 mice (B6-*gfp/luc*) were bred in our animal facility at Stanford University. FoxP3.Luci.DTR-4 mice (B6-albino background, the expression of luc/gfp proteins were controlled by the *foxp3* promoter) were provided by Gunther Hammerling, Heidelberg, Germany.[13] Littermate WT-B6 albino mice were used as controls. C57BL/6-Foxp3-DTR mice (B6-Foxp3DTR mice) were provided by Alexander Rudensky, Memorial Sloan Kettering Cancer Center, New York, NY. Mice were used between the age of 8 and 16 weeks, and sex-matched combinations were used for transplant experiments. All animal protocols were approved by the Institutional Animal Care and Use Committee at Stanford University.

Antibodies and reagents

The FcR blocking reagent, magnetic microbeads, and LS columns were purchased from Miltenyi Biotec (Auburn, CA). Agonistic anti-DR3 Ab (clone: 4C12) and hamster immunoglobulin G isotype control Ab were purchased from Biolegend (San Diego, CA). All antibodies for flow cytometric analysis were purchased from Biolegend or eBioscience (San Diego, CA). Fixable Viability Dye eFluor 506 (eBioscience) was used to exclude dead cells. FoxP3 Fixation/Permeabilization buffer set was purchased from eBioscience. Diphtheria toxin for Treg depletion was purchased from Sigma-Aldrich. All assays were performed with an LSR II cytometer (BD Biosciences). For the comprehensive multicolor analysis, single-color staining and UltraComp eBeads (eBioscience) were used for the adjustment of compensation. FMO (fluorescence minus one) samples were used for positive gating. All data were analyzed using FlowJo software (TreeStar, Ashland, OR) and Cytobank (www.cytobank.org).[14,15]

Cell isolation and sorting

αDR3 or isotype control Ab was administered by intraperitoneal injection at a dose of 0.5 mg/kg of body weight. Whole splenocytes were isolated and T cells were purified by magnetic activated cell sorting (MACS), using anti-CD4 and anti-CD8 microbeads. For CD25$^+$ Treg isolation, cells were stained with anti-CD25 APC, incubated with anti-APC microbeads, and positively selected with an LS column, as previously described[16]

TCR stimulation and mixed lymphocyte reaction

MACS-purified T cells (2×10^5/well) were cultured with RPMI and stimulated with Mouse T-activator CD3/CD28 beads (Gibco) at various ratios (from 1:10 to 1:20). CellTrace Violet (Molecular Probes) was used for visualization of T-cell proliferation according to the manufacturer's protocol. In mixed lymphocyte reaction (MLR) culture, T cells from WT-B6 or B6 albino mice were cocultured with γ-irradiated (3000 cGy) Balb/c splenocytes (2×10^5/well) as stimulator cells. After 96 hours, cells were pulsed with [^{3}H] thymidine (1 μCi/well) for 16 hours. [^{3}H] thymidine incorporation was measured with a Wallac Betaplate counter (Perkin-Elmer).

Bioluminescence imaging

In vivo bioluminescence imaging (BLI) was performed as described previously.[17] Briefly, the mice were injected intraperitoneally with luciferin (10 μg/g body weight), anesthetized, and imaged using an IVIS Spectrum charge-coupled device imaging system (Caliper-Xenogen, Alameda, CA) for up to 5 minutes. Imaging data were analyzed with Living Image Software (Caliper Life Sciences, Hopkinton, MA).

Multiplex cytokine assays

Sera were collected from the recipient mice on day 7 after transplant. Twenty different cytokines were analyzed in a multiplex assay system (Cytokine Mouse 20-plex Panel for the Luminex platform, LMC0006; Invitrogen, Carlsbad, CA) and quantitated using the Luminex 200 system (Luminex, Austin, TX).

Fluorescence microscopy

Tissue samples were harvested from the recipient mice 7 days after transplant. Five-micrometer-thickness cryosections were prepared. Slides were fixed with 4% paraformaldehyde, stained with DAPI, and observed on a fluorescence microscope (Olympus BX41, Center Valley, PA). Images were analyzed by Image J (1.47v; National Institutes of Health).

Microarray analysis

Total RNA from purified Treg were isolated using RNAeasy Minikit (Qiagen). RNA quality was assessed by Agilent 2100 BioAnalyzer (Agilent). Hybridization to Mouse Gene 2.0 ST array (Affymetrix), processing, and scanning were performed by Filgen (Nagoya, Japan). Data were normalized using the robust multichip analysis normalization method.[18] Microarray Data Analysis Tool version 3.2 was used for drawing scatter plots, and *t* test and hierarchical clustering for microarray data were performed using MultiExperiment Viewer (MeV, version 4.9). Correction for multiple comparisons was performed using the Benjamini-Hochberg method with false recovery rate < 0.1. Gene expression data sets can be accessed at the National Center for Biotechnology Information and Gene Expression Omnibus database (http://www.ncbi.nlm.nih.gov/geo; accession number GSE83743).

Statistical analysis

Survival curves were plotted with the Kaplan-Meier method and compared by a log-rank test. Data were displayed with mean and SEM on a bar or scatter dot plot. The multiple *t* tests and 2-tailed Student *t* test were performed by Prism 6 (GraphPad Software, La Jolla, CA).

Results

Regulatory T cells activated thorough DR3 signaling have a distinct immunophenotype

To investigate whether the stimulation of Treg through DR3 signaling would affect the immune phenotype and function of Treg, we analyzed the expression level of a panel of activation molecules/transcriptional factors in CD4$^+$Foxp3$^-$ T cells, CD8$^+$ T cells, and Treg after αDR3 or isotype control Ab treatment of WT B6 mice (Figure 1A). As expected, the frequencies of Foxp3$^+$ cells among CD4$^+$ cells and Ki67$^+$ expression (proliferation marker) in Treg were significantly increased (Figure 1A; supplemental Figure 1B, available on the *Blood* Web site). Interestingly, the expression of activation molecules including Lag3, TIGIT, PD1, and LAP (TGF-β1) in Treg were significantly elevated in Treg exposed to αDR3 compared with isotype control Ab treatment (Figure 1Ai). Helios and Nrp1 (transcription factor and surface molecule for recent thymic emigrants),[19,20] as well as CD103 and KLRG1 (maturation markers),[21,22] were also elevated in αDR3-treated Treg (DR3-Treg; Figure 1Ai). CD25, the receptor for interleukin 2, was downregulated in DR3-Treg, as previously reported (Figure 1Ai). In CD4$^+$Foxp3$^-$ T cells and CD8$^+$ T cells, we also observed statistically significant elevations of these molecules (Figure 1Aii-iii), although the

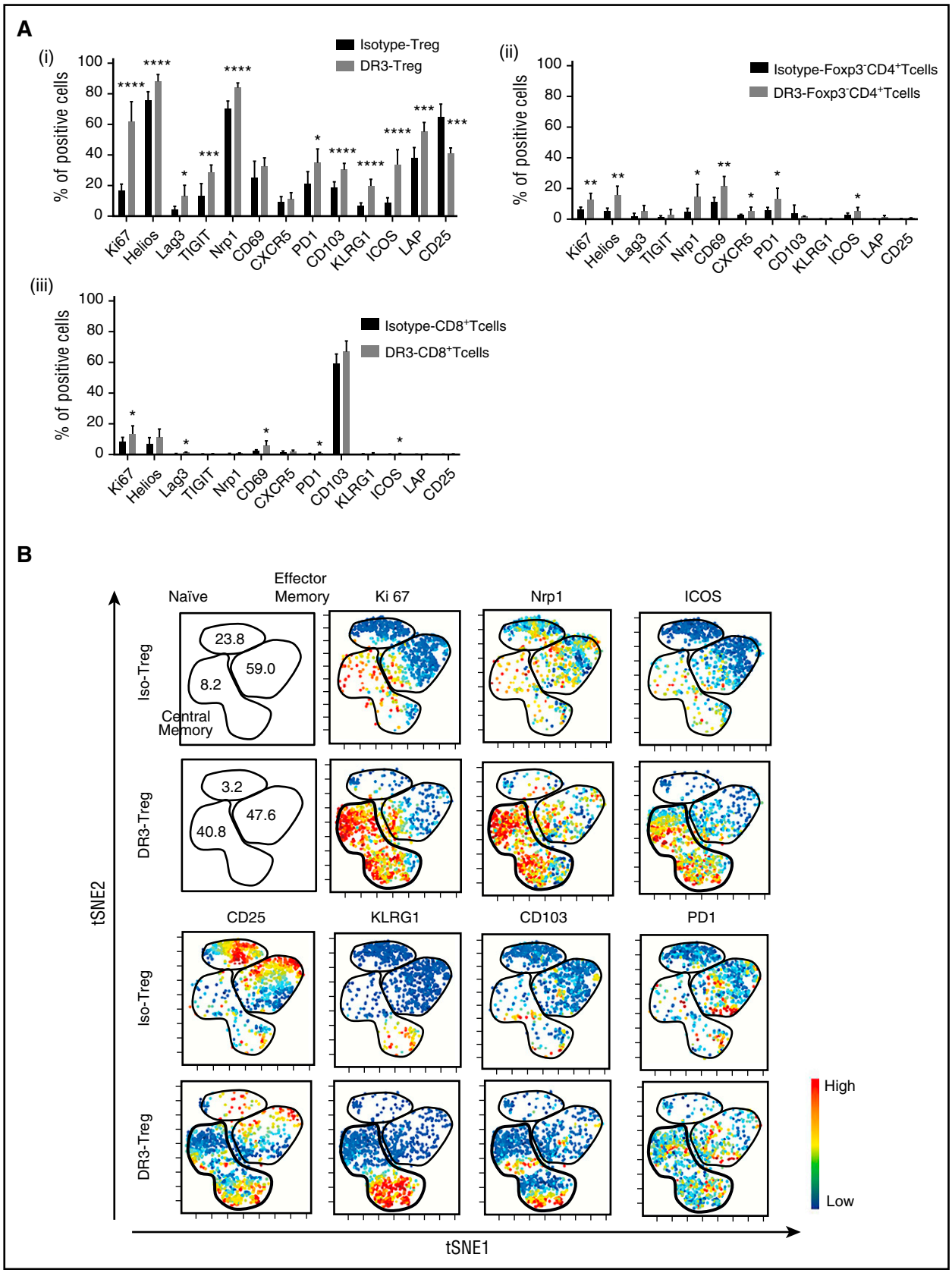

Figure 1. Treg expanded through DR3 signaling show a distinct immunophenotype. Whole T cells were isolated from αDR3 or isotype control Ab-treated WT-B6 mice and analyzed by FACS at 4 days after treatment. (A) The expression level of activation molecules in Foxp3$^+$Treg (i), CD4$^+$Foxp3$^-$Tcells (ii), CD8$^+$ T cells (iii) after in vivo expansion through DR3 signaling (n = 5; $^*P < .05$; $^{**}P < .01$; $^{**}P < .001$; $^{****}P < .0001$). (B) The representative results of viSNE analysis using multicolor cytometry data in isotype control Ab-treated Foxp3$^+$Treg (Iso-Treg) and αDR3-treated Foxp3$^+$ Treg (DR3-Treg). The colors were scaled to the expression level of each molecule as indicated.

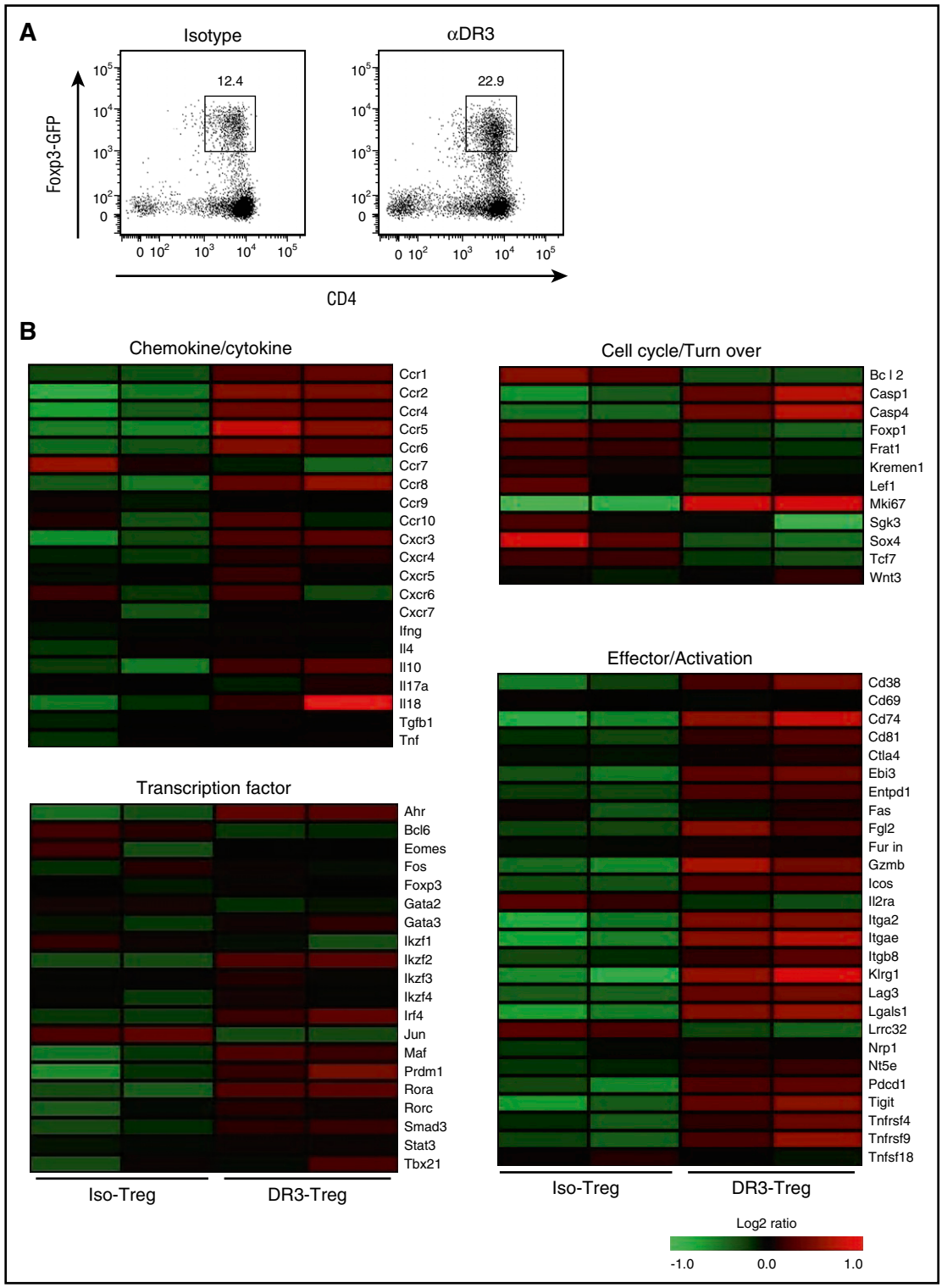

Figure 2. DR3-activated Foxp3$^+$Tregs show a distinct gene expression profile. (A) The gating strategy for Treg isolation from FoxP3.Luci.DTR-4 mice. (B) Gene expression profiles of Iso-Treg and DR3-Treg. The expression changes in chemokine/cytokine, transcription factor, cell cycle/turn over and effector/activation molecules are shown as a heat map, where red and green represent the highest- and lowest-expressed genes, respectively.

effect of αDR3 in these populations was much less than in Treg. These data suggested that activation through DR3 signaling could not only expand but also preferentially activate Treg.

We previously demonstrated that Treg expanded after DR3 activation showed a CD62L$^+$CD44$^+$ central memory phenotype (supplemental Figure 1C).[11] viSNE analysis (visualization of stochastic neighbor embedding) enables one to map high-dimensional cytometry data onto 2 dimensions, yet conserve the high-dimensional structure of the data.[15] Using this novel method to analyze multiparameter data in DR3-Treg (14-color staining using anti-CD4, CD8, Foxp3, CD25,

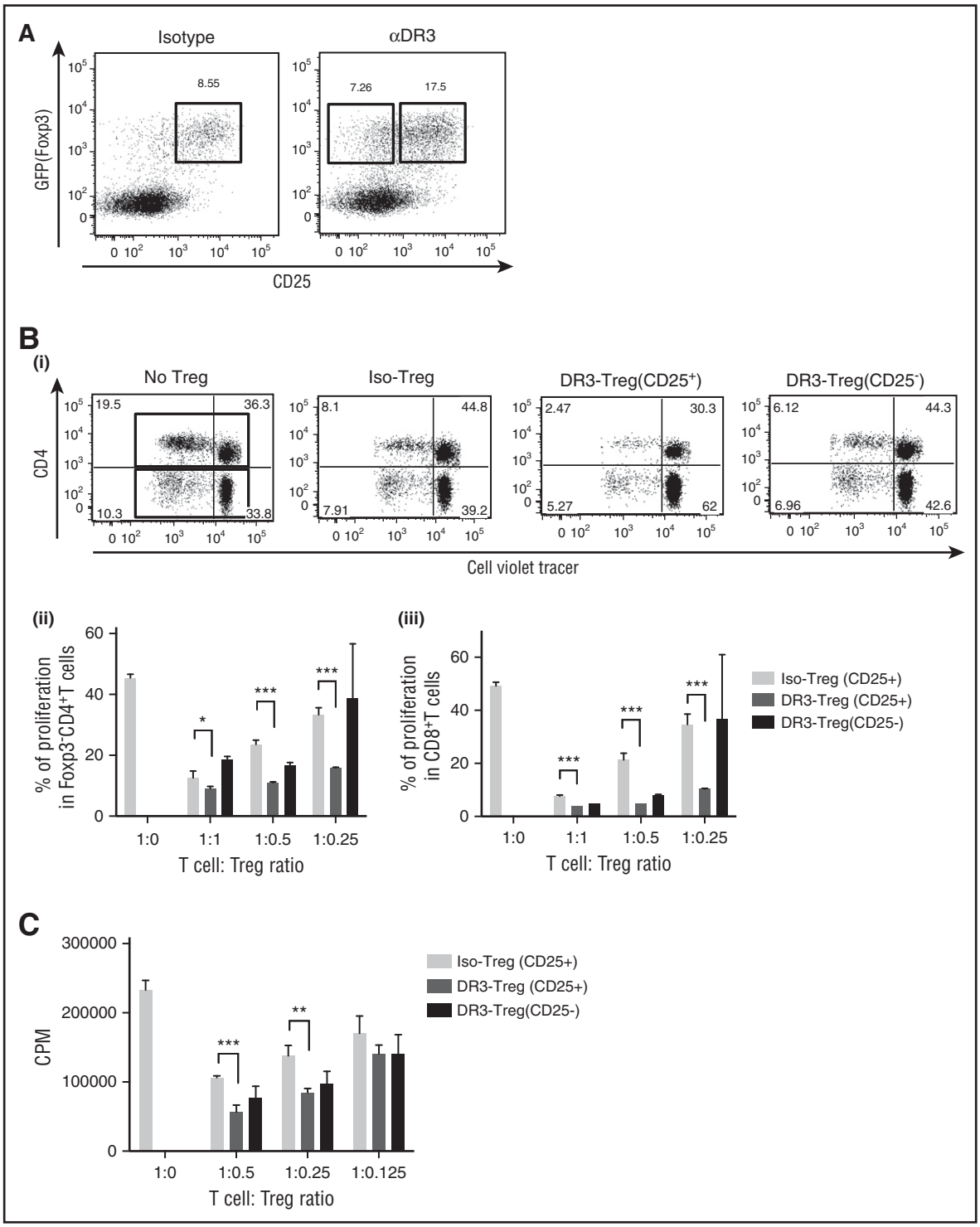

Figure 3. CD25$^+$ Foxp3$^+$ Treg after DR3 activation retain suppressive effects in TCR mediated T-cell proliferation. CD4$^+$CD25$^+$Foxp3$^+$ Treg were isolated from αDR3 or isotype control Ab-treated mice and cultured with freshly isolated T cells (2×10^5) from untreated mice. (A) The gating strategy for CD25$^+$ Treg isolation from Foxp3-Luci4 mice. (B) T cells were tagged with CVT and cultured with CD3/CD28 beads, together with isolated Treg. (i) The representative plots of proliferating T cells tagged with CVT were shown. (ii-iii) The frequencies of proliferating (CVT ^{dim}) CD4$^+$Foxp3$^-$ (ii) and CD8$^+$ T cells (iii) were analyzed by FACS (n = 6; $^*P < .05$; $^{***}P < .001$). (C) MLR using freshly isolated T cells from nontreated WT-B6 albino mice and γ-irradiated splenocytes from Balb/c mice with or without isolated Treg was performed. [^{3}H] thymidine incorporation was measured and analyzed ($^{**}P < .01$; $^{***}P < .001$). The representative data of 2 independent experiments (each experiments were triplicate) are shown ($^{**}P < .01$, $^{***}P < .001$).

CD62L, CD44, Ki67, PD1, CD103, Nrp1, ICOS, Lag3, KLRG1, and viability dyes), we next comprehensively analyzed the immune phenotype of DR3-Treg (Figure 1B; supplemental Figure 1). Ki67$^+$-expressing Treg were located in the central memory phenotype of Treg, as expected. The pattern of Nrp1, ICOS, and PD1-positive Treg activated with αDR3 also were preferentially within the central memory

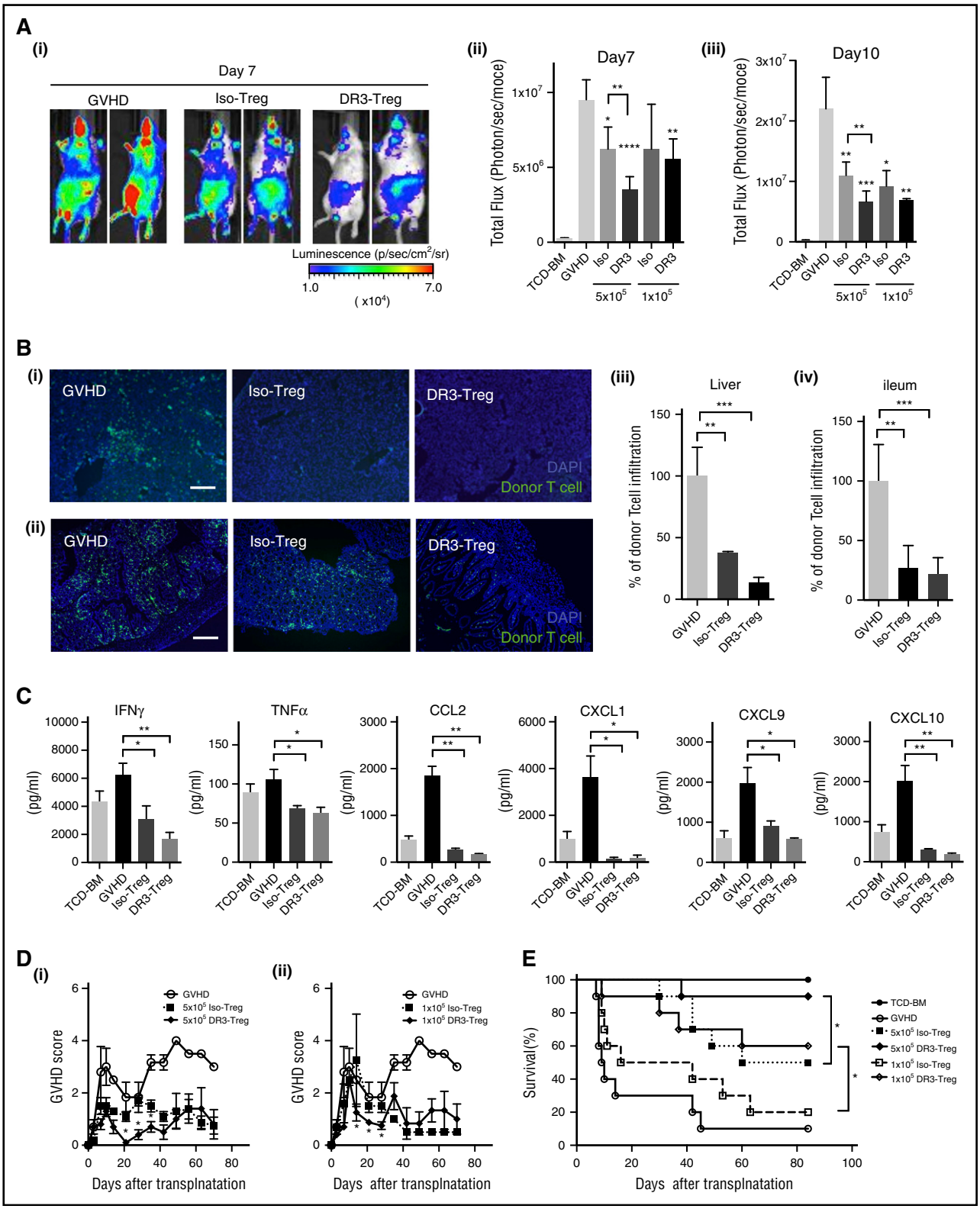

Figure 4. Expanded CD25$^+$Foxp3$^+$ Treg after DR3 activation prevent acute GVHD after allogeneic transplantation. CD4$^+$CD25$^+$ Treg (1×10^5-5×10^5/animal) from WT B6 mice with or without αDR3 treatment were transplanted together with T cells from B6-*gfp/luc* mice (1×10^6/animal) and TCD-BM from WT B6 mice into lethally irradiated Balb/c mice. (A) Donor T-cell proliferation in vivo was measured by BLI. Representative BLI image of GVHD control (left), Iso-Treg group (middle), and DR3-Treg group (right) on day 7 are shown. The summary of BLI on day 7 (ii) and day 10 (iii) are shown (n = 5; *$P < .05$; **$P < .01$; ***$P < .001$; ****$P < .0001$). (B) Representative immunohistochemistry images of liver (i) and ileum (ii) samples from transplanted mice on day 7 are shown (n = 3, green, donor T cells (GFP); blue, DAPI; scale bar, 200 μm). The frequencies of infiltrating donor GFP$^+$ T cells into the tissue were calculated (iii-iv; n = 3; **$P < .01$; ***$P < .001$; ****$P < .0001$). (C) Serum inflammatory cytokine/chemokine levels (interferon γ, TNFα, CCL2, CXCL1, CXCL9, CXCL10) from transplanted mice are shown (n = 4 in each group; *$P < .05$; **$P < .01$). D-E. GVHD score and survival were assessed (n = 10 in each group; *$P < .05$).

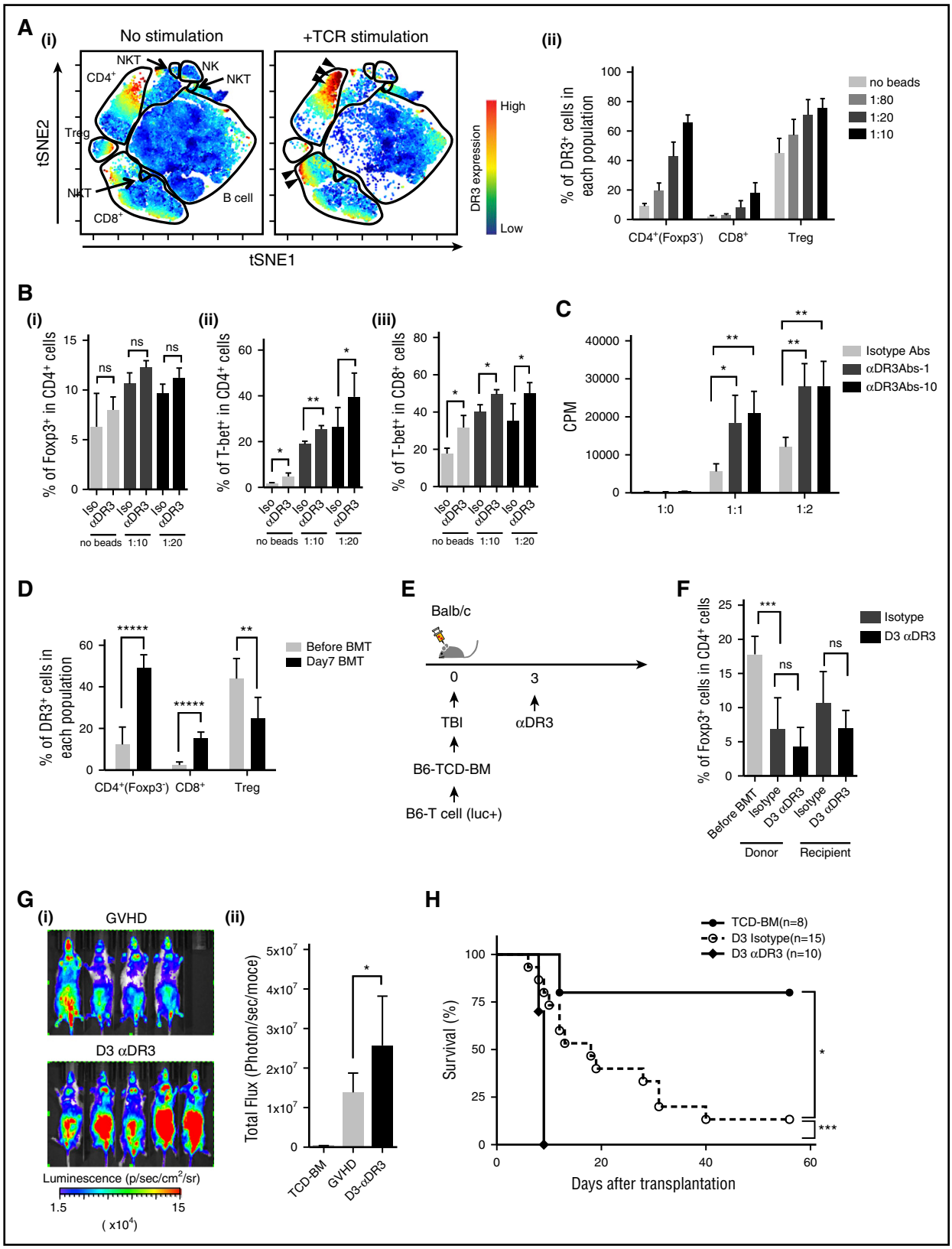

Figure 5. DR3 activation after alloantigen exposure promotes donor T-cell activation. (A, i) Representative results of DR3 expression in immune cells by viSNE analysis are shown. Whole splenocytes were isolated and stained with various antibodies. $CD4^+$ T cells ($CD4^+TCR\beta^+Foxp3^-$), $CD8^+$ T cells ($CD8^+TCR\beta^+$), B cells ($TCR\beta^-B220^+$), NK cells ($NK1.1^+TCR\beta^-B220^-$), NKT cells ($NK1.1^+TCR\beta^+$), and Treg ($CD4^+TCR\beta^+Foxp3^+$) were categorized as shown in the panel (supplemental Figure 4). The colors were scaled to the expression level of DR3. (ii) The expression level of DR3 in $CD4^+Foxp3^-$ T cells, $CD8^+$T cells, Treg after CD3/CD28 beads activation at various ratios (T cells:beads 1:80-1:10) are shown (n = 6). (B) T cells were cultured with CD3/CD28 beads together with αDR3 or isotype control Abs. After 3 days in culture, Foxp3 (i) and T-bet (ii-iii) expression were analyzed (n = 6; ns = not significant; $*P < .05$; $**P < .01$). (C) MLR using freshly isolated T cells from nontreated WT B6 mice and γ-irradiated splenocytes from WT Balb/c mice with or without αDR3 (1-10 μg/mL) was performed. The ratio of responder (T cell):stimulator (irradiated splenocytes) was from 1:0 to 1:2, as

phenotype. The subpopulation of central memory phenotype Treg expressed KLRG1 and CD103. These data also supported that Treg expanded after DR3 activation showed an activated immunophenotype. To confirm that these phenotypic changes preferentially occurred within the Treg population, viSNE analyses were also performed using whole T cells (supplemental Figure 2). The results of the viSNE map demonstrated that these immunophenotypic changes preferentially occurred in Treg, as compared with the $CD4^+Foxp3^-$ and the $CD8^+$ T-cell population.

DR3-activated Treg showed distinct gene expression profiles

Next, we treated FoxP3.Luci.DTR-4 mice with αDR3, sorted $Foxp3^+$ Treg 4 days after treatment, and analyzed gene expression profiles (Figure 2; supplemental Figure 3). The 33793 probe sets were analyzed and compared with isotype control Abs treated Treg (Iso-Treg) and DR3-Treg (supplemental Figure 3A). In both groups, the expression of *foxp3* was comparable and at high level (supplemental Figure 3C), confirming that Treg were appropriately sorted. We next selected several genes (22 chemokine/cytokines, 20 transcription factors, 12 cell cycle/turn over molecules, 27 effector/activation molecules) to characterize DR3-Treg; Figure 2B; supplemental Figure 3B-E).[22,23] Using a heat map analysis, DR3-Treg expressed chemokine and effector molecules at higher levels compared with Iso-Treg (Figure 2B; supplemental Figure 1B-E). Statistically significant differences in several chemokine/cytokine/chemokine receptors for tissue migration (*ccr2*, *ccr4*, *ccr8*) were observed (*t* test $P < .05$; false recovery rate <0.1; supplemental Table 1). The transcript level of interleukin 10, a major suppressive cytokine from Treg, trended toward higher expression in DR3-Treg, but did not reach statistical significance (Figure 2B; supplemental Figure 3B). Suppression molecules in Treg (*Gzmb*, *Fgl2*, *lag3*, *Ebi3*, *Entpd1*, *ctla4*) were expressed at statistically higher levels in DR3-Treg (Figure 2B; supplemental Table 1). Among the cell cycle/apoptosis related genes, significantly higher levels of *Ki67* in DR3-Treg were observed, consistent with protein expression (Figure 1; Figure 2; supplemental Table 1). Maturation molecules of Treg (*Klrg1*, *itgae*) were also expressed in DR3-Treg at higher levels. Pro-apoptotic molecules, *Casp1* and *Casp4,* were expressed at significantly higher levels in DR3-Treg. However, the anti-apoptotic molecule, *Bcl2,* was significantly downregulated in DR3-Treg. These data suggested that DR3-Treg showed an activated phenotype.

DR3-activated Treg have enhanced function

We next analyzed functional characteristics of the DR3-Treg to clarify the effect of DR3 signaling (Figure 3). CD25 is one of the markers for mouse Treg isolation,[16] although DR3-Treg showed lower expression levels of CD25 (Figure 1; Figure 3A). Therefore, we isolated $CD25^+$ Iso-Treg, $CD25^+$DR3-Treg, and $CD25^-$DR3-Treg and analyzed their suppressive effects on T-cell proliferation. Cell violet tracer (CVT)–labeled T cells from WT-B6 albino mice were cocultured with isolated Treg at various ratios and stimulated with CD3/CD28 beads (Figure 3B). After 72 hours of culture, the cells were harvested and analyzed for the frequencies of proliferating CVT^{dim} T cells by flow cytometry. As expected, the proliferation of CVT-tagged T cells cocultured with Iso-Treg was inhibited compared with those without Treg (Figure 3B). Interestingly, $CD25^+$ DR3-Treg showed more profound suppressive effects on proliferation of conventional $CD4^+$ and $CD8^+$ T cells (Figure 3Bii-iii). $CD25^-$DR3-Treg also inhibited T-cell proliferation (Figure 3B); however, their suppressive effects were less than $CD25^+$DR3-Treg, especially at lower numbers of cells (Figure 3Bii-iii; T cell:Treg ratio 1:0.25). $CD25^+$DR3-Treg also showed stronger suppressive effects of allogeneic T-cell proliferation compared with Iso-Treg in allogeneic MLR culture (Figure 3C).

Next, we performed transplant experiments to clarify whether DR3-Treg retained function in controlling GVHD in murine model of allogeneic HCT. BLI was used to evaluate donor T-cell proliferation and trafficking. WT-Balb/c mice that received $CD25^+$DR3-Treg (from WT B6 mice, 5×10^5/mouse) showed significantly lower donor T-cell (from B6 *gfp/luc*$^+$ mice, 1×10^6/mouse; Figure 4A) proliferation compared with the mice who received Iso-Treg (n = 5 in each group; $P < .01$ on days 7 and 10 after transplant; Figure 4Ai-iii). Interestingly, even a smaller number (1×10^5/mouse) of $CD25^+$DR3-Treg suppressed donor T-cell proliferation in recipient mice (n = 5 in each group; $P < .01$ on days 7 and 10; Figure 4Aii-iii). To investigate donor T-cell infiltration into GVHD target tissues, we also isolated the liver and small bowel (distal ileum) from transplanted mice on day 7 and analyzed the frequencies of infiltrated donor-derived GFP^+ T cells into tissues (Figure 4B). Consistently, donor T-cell infiltration into the periportal area in the liver (Figure 4Bi) and mucosa in the small bowel (Figure 4Bii) was significantly lower in DR3-Treg group compared with the control GVHD group (Figure 4Biii-iv; $P < .01$; $P < .001$), and the frequencies of donor T-cell infiltration into liver in the DR3-Treg group were statistically lower than those in the Iso-Treg group (Figure 4Biii; $P < .0001$).

We also analyzed the concentrations of serum cytokines and chemokines, which play an important role in the pathophysiology of GVHD (Figure 4C). The serum levels of proinflammatory cytokines, such as interferon γ and TNFα, were significantly lower than control GVHD animals ($P < .05$; $P < .01$). The level of chemokines, such as CCL2, CXCL1, CXCL9, and CXCL10, were also reduced in Treg-treated groups, which were consistent with previous studies.[11]

As expected, the mice treated with Treg showed lower GVHD scores and better survival compared with the control GVHD group (Figure 4D-E). When compared between the Iso-Treg- and the DR3-Treg-treated group, the mice that received DR3-Treg had significantly lower GVHD scores than the mice treated with Iso-Treg (Figure 4D). Survival of the mice that received DR3-Treg was also improved compared with Iso-Treg group (n = 10 in each group; $P < .05$ in Log-rank test), even with a suboptimal number (1×10^5) of Treg (Figure 4E). These data demonstrate that Treg isolated after DR3 activation are more functional for the prevention of GVHD after allogeneic HCT.

DR3 signaling promotes donor T-cell activation after alloantigen exposure

We next investigated whether αDR3 treatment of recipient mice can expand recipient-derived Treg or modulate the severity of GVHD. We

Figure 5 (continued) shown in the graph. [^{3}H] thymidine incorporation was measured and analyzed (*$P < .05$; **$P < 0.01$; ***$P < .001$). Representative data from 2 independent experiments (each experiment was performed in triplicate) are shown. (D) T cells were isolated from the GVHD mice on day 7. DR3 expression on donor T cells was analyzed (n = 5; **$P < .01$; ****$P < .0001$). (E) TCD-BM from WT B6 mice and T cells from B6-*luc* mice were transplanted into lethally irradiated Balb/c mice on day 0. αDR3 or isotype control Ab was injected on day 3. (F) T cells from the spleen were isolated on day 7 after transplant, and the frequencies of $Foxp3^+$ cells from donor- or recipient-derived $CD4^+$ T cells were analyzed (n = 4; ns = not significant; ***$P < .001$). (G) Donor T-cell proliferation in mice treated on day 3 with αDR3 was assessed by BLI. Representative images on day 7 are shown in (i). The summary of BLI was shown in (ii) (n = 10; *$P < .05$). (H) Survival curve is assessed (*$P < .05$; ***$P < .001$).

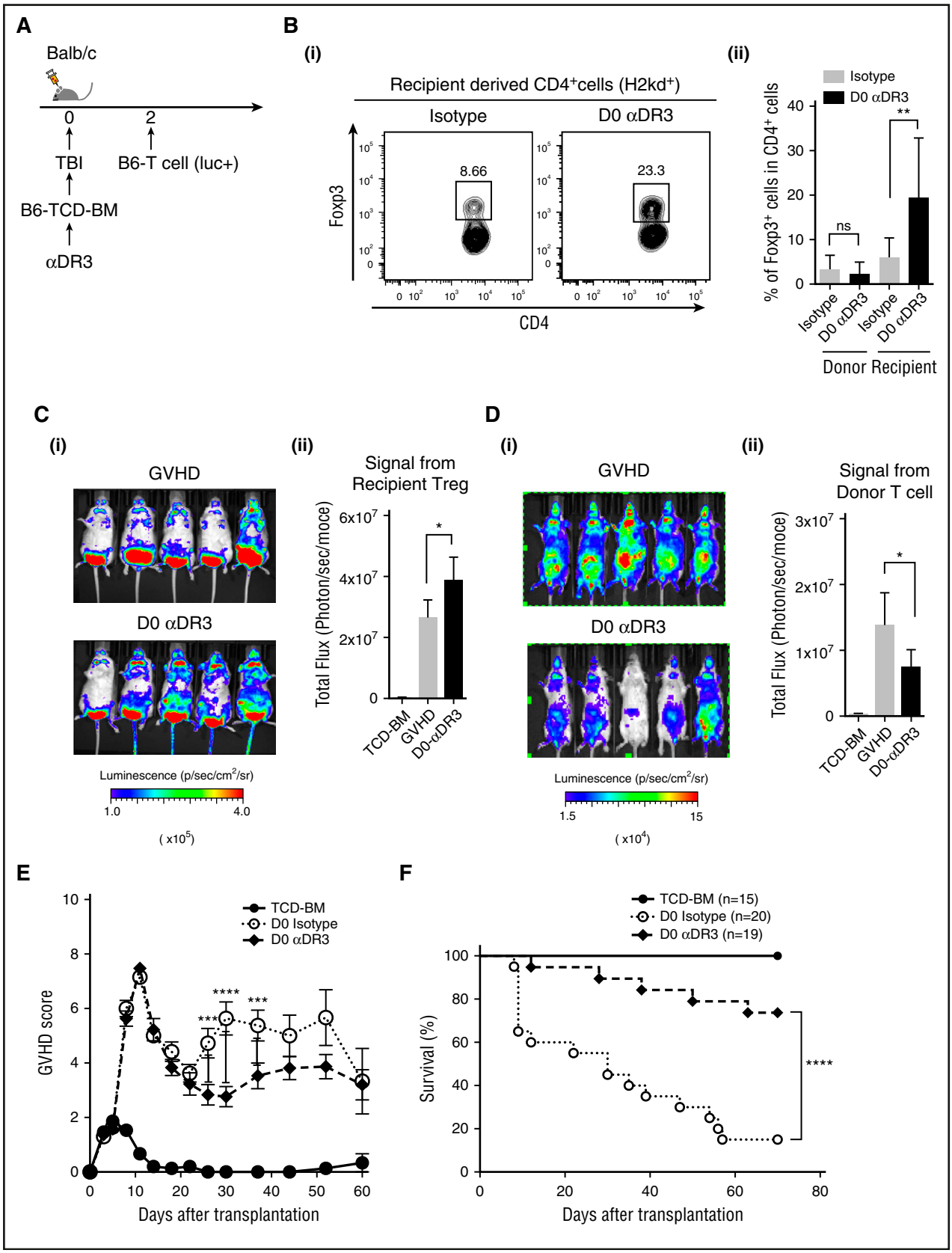

Figure 6. DR3 activation before alloantigen exposure promotes recipient-derived Treg expansion and prevented acute GVHD. (A) TCD-BM from WT B6 mice were transplanted into lethally irradiated Balb/c recipients on day 0, and T cells from B6-*luc* mice (1×10^6/animal) were injected on day 2 after transplant to induce acute GVHD. αDR3 or isotype control Ab was injected on day 0. (B) Splenic T cells were isolated on day 7 after transplant and the frequencies of Foxp3$^+$ cells in donor- or recipient-derived CD4$^+$ T cells were analyzed by FACS. (i) Representative dot plot data of recipient-derived CD4$^+$T cells were shown. (ii) The summary of statistical analysis were shown (n = 7; n.s. = not significant; $^{**}P < .01$). (C) Recipient-derived Treg proliferation with or without D0 αDR3 treatment was assessed using lethally irradiated (9.5 Gy) Foxp3-Luci4 mice

first analyzed the surface expression of DR3 in immune cells after T-cell activation. In viSNE analysis, using splenocytes derived from normal mice, Treg had higher levels of expression of DR3 (79%) than $CD4^+$ $Foxp3^-$ T cells (59%), $CD8^+$ T cells (24%), or $TCR\beta^+NK1.1^+$ NKT cells (42%) (Figure 5Ai, left; supplemental Figure 4). In bone marrow cells, the expression pattern was essentially same as in the splenocytes (data not shown). We then analyzed DR3 expression on T cells incubated with CD3/CD28 beads in vitro at various ratios (Figure 5Ai-ii). After 3 days of culture, DR3 expression on $CD4^+Foxp3^-$ T cells and $CD8^+$ T cells were significantly elevated in a dose-dependent manner, implying that DR3 expression was affected by the activation status in both Treg and non-Treg populations (Figure 5Ai, right; Fig 5Aii). Next, T cells were cultured at various ratios of CD3/CD28 beads with or without αDR3 (Figure 5B-C). As previously reported,[10] the frequency of $Foxp3^+$ cells in $CD4^+$ T cells were not significantly changed (Figure 5Bi). Instead, we observed a significant elevation of T-bet, a known marker for T helper 1, in $CD4^+$ T cells (Figure 5Bii) and $CD8^+$ T cells (Figure 5Biii). We then analyzed donor T-cell proliferation in MLR cultures with or without αDR3 (Figure 5C). Donor T-cell proliferation was promoted by αDR3 treatment, suggesting DR3 signaling could affect allogeneic stimulation in donor T cells through TCR activation.

In mice with GVHD, DR3 expression on donor $CD4^+Foxp3^-$ T cells and $CD8^+$ T cells were significantly elevated, whereas DR3 on Treg was downregulated (Figure 5D), suggesting the effect of αDR3 in mice with GVHD might be different from that in normal mice. To investigate the effects of αDR3 on mice with acute GVHD, we injected αDR3 (day 3 after transplant) into mice that received T-cell–depleted bone marrow (TCD-BM) and *luc*$^+$T cells on day 0 (Figure 5E-G). In this setting, we did not observe Treg expansion of either the donor- or recipient-derived $CD4^+$ T cells (Figure 5F). Instead, donor T-cell proliferation in vivo was significantly promoted by αDR3 treatment (Figure 5Gi-ii). Acute GVHD was enhanced in αDR3-treated mice, and these animals died within 2 weeks after transplant (Figure 5H). These data suggested that αDR3 treatment to the mice with ongoing GVHD promoted donor T-cell proliferation and activation and failed to result in Treg expansion.

DR3 activation before T-cell activation expands recipient-derived Treg and suppresses GVHD

Activation through DR3 signaling in mice with acute GVHD enhanced donor T-cell proliferation/activation and promoted GVHD (Figure 5), whereas robust functional Treg expansion could be observed when we treated steady-state mice (Figures 1-4).[10,11] To investigate whether prophylactic treatment with αDR3 could expand Treg and reduce the severity of acute GVHD, we next administered αDR3 to the recipient mice before allogeneic T-cell injection (Figure 6A). αDR3 was administered to WT Balb/c recipient mice that were subsequently irradiated and transplanted with TCD-BM (from WT B6 mice) on day 0, and allogeneic T cells (from B6-*luc* mice, 1×10^6 cells) injected on day 2 after transplant (Figure 6A). To clarify whether αDR3 could expand donor- or recipient-derived-Treg, splenocytes were isolated on day 5 after transplant (Figure 6B). Interestingly, the frequency of recipient-derived Treg ($H2kd^+CD4^+Foxp3^+$ cells) were increased in the mice treated with αDR3 (Figure 6B), whereas donor-derived Treg ($H2kb^+CD4^+Foxp3^+$ cells) did not show any significant change (Figure 6Bii). We also confirmed the proliferation of recipient-derived Treg after day 0 αDR3 treatment, using lethally irradiated Foxp3-Luci4 recipient mice and WT Balb/c donor mice (Figure 6C). Moreover, when donor T-cell infiltration in the recipient mice was assessed by BLI (Figure 6D) on day 7 after transplant, the recipient mice treated with αDR3 showed lower signal assessed by BLI than those animals treated with isotype control Ab (Figure 6D). GVHD score and survival in each group were also assessed (Figure 6E-F). GVHD score in αDR3 treated mice was significantly lower than animals in the isotype control Ab-treated group, although there were no statistical differences at early points after transplant (from day 0 to day 21; Figure 6E). There was a significant survival benefit in animals treated with αDR3 on D0 before allogeneic T-cell injection (Figure 6F). Considering the results that αDR3 treatment to the mice with ongoing GVHD failed to expand Treg and activate donor T cells (Figure 5), the effect of DR3 activation in GVHD is highly dependent on the activation status of the donor T cells and the timing of administration.

To investigate whether the prophylactic effects of αDR3 were dependent on the activity of donor- or recipient-derived Treg, we used B6-Foxp3 DTR mice as either donor or recipients and depleted Treg with diphtheria toxin (DT). To deplete Treg from the donor T cells (Figure 7Ai), DT was injected to donor mice on day −2 and day −1.[24] T cells were then isolated from Treg-depleted donor mice and transplanted into lethally irradiated WT-Balb/c mice. Mice treated with αDR3 on day 0 demonstrated a significantly lower GVHD score at later points after transplant (Figure 7Aii). Despite depletion of donor-derived Treg, there was still a significant survival benefit in animals treated with αDR3 on day 0 before transplantation (Figure 7Aiii). These data suggested that donor-derived Treg are not responsible for the improved survival observed after αDR3 treatment on day 0.

Next, B6-Foxp3 DTR mice were used as recipients, and DT was injected on day 2, day 1, day 3, and day 5. Recipient mice were irradiated on day 0, followed by injection of TCD-BM. T cells isolated from WT-Balb/c mice were injected on day 2 (Figure 7Bi). Depletion of host Treg with DT resulted in significantly higher GVHD scores and death within 3 weeks after transplant, even with day 0 αDR3 treatment (Figure 7Bii; TCD-BM + T cell + day 0 αDR3 vs TCD-BM + T cell + day 0 αDR3+DT; $P < .001$), and the survival benefit of day 0 αDR3 treatment was no longer observed when recipient-derived Treg were depleted (Figure 7Biii; TCD-BM + T cell + day 0 αDR3 vs TCD-BM + T cell + day 0 αDR3+DT; $P < .001$; TCD-BM + T cell + DT vs TCD-BM TCD-BM + T cell + day 0 αDR3+DT; P = n.s). These data indicate that recipient derived Treg play a critical role in protecting lethal GVHD after the prophylactic treatment of animals with αDR3. Taken together, we conclude that prophylactic treatment with αDR3 to recipient mice activated and expanded recipient-derived Treg and that they were required for the observed reduction in lethal GVHD.

Discussion

Regulatory T cells have been shown to be biologically active in a variety of model systems of autoimmune diseases, transplantation tolerance induction, and GVHD suppression. In the setting of allogeneic HCT, Treg have been shown to suppress GVHD in a number of different strain combinations, yet promote immune reconstitution

Figure 6 (continued) as recipients. Representative images on day 7 are shown (i). Summary of BLI (ii) (n = 10; *$P < .05$). (D) Donor T-cell proliferation (from B6-*luc* mice) in the recipient mice (WT Balb/c mice) with or without D0 αDR3 treatment was assessed by BLI. Representative images on day 7 are shown (i). Summary of BLI is shown in (ii) (n = 10; *$P < .05$). (E-F) GVHD score and survival curve are shown (*** $P < .001$; ****$P < .0001$).

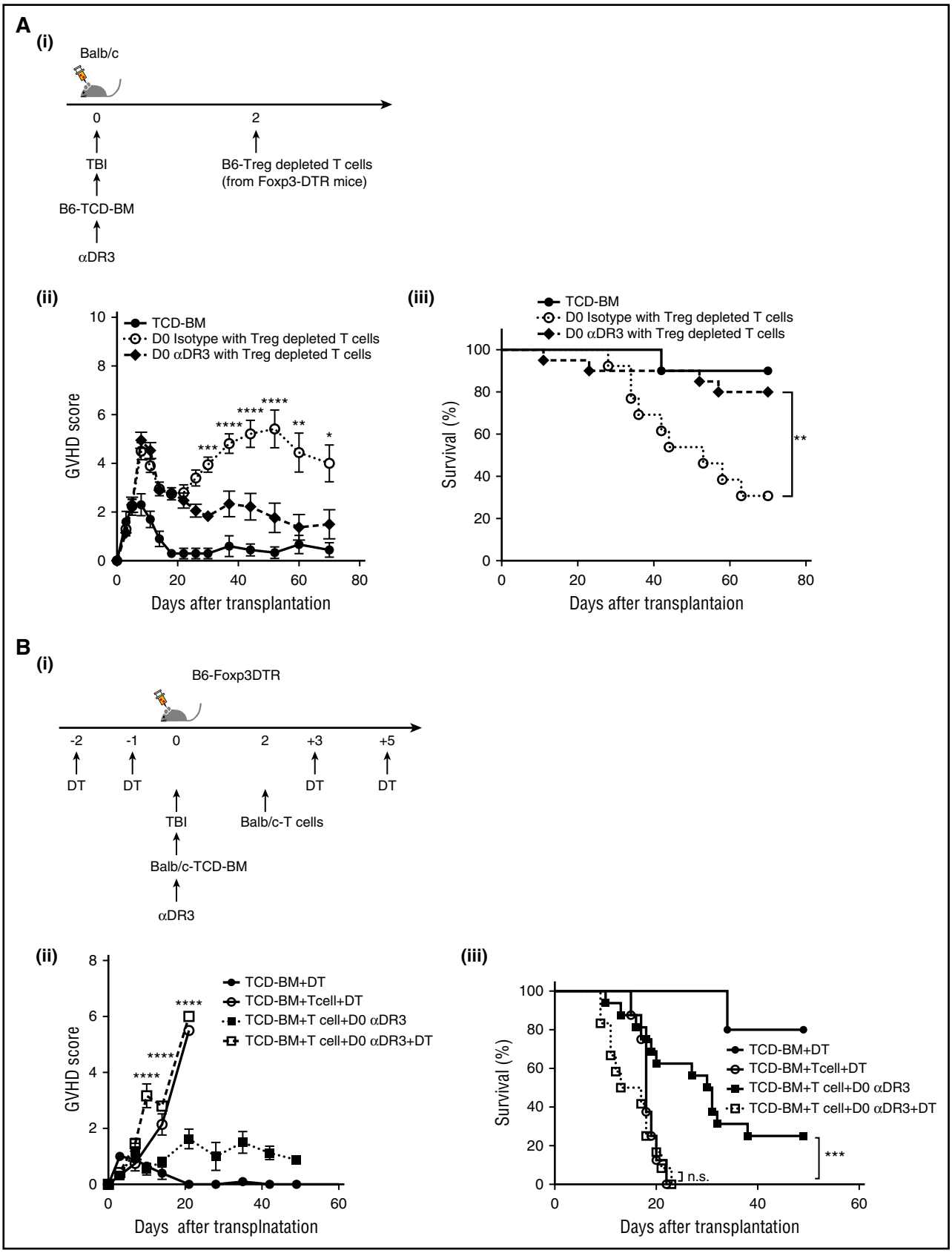

Figure 7. The efficacy of prophylactic treatment with DR3 activation is dependent on recipient-derived Treg. (A) TCD-BM from WT B6 mice were transplanted into lethally irradiated Balb/c recipients on day 0, and Treg-depleted T cells from B6-Foxp3DTR mice (1×10^6/animal) were injected on day 2 after transplant. For preparation of Treg-depleted T cells, DT (1 μg/animal) was administered to donors on days −2 and −1. αDR3 or isotype control Ab was injected into recipient mice on day 0. (i) Experimental scheme. GVHD score (ii) and survival curve (iii) are shown (n = 10 in TCD-BM; n = 13 in D0 isotype with Treg-depleted T cells; and n = 20 in D0 αDR3 with

without any adverse effects on GVT reactions.[17,25-27] Because of these attractive biological functions, there has been great interest in translation to the clinic, and early clinical trials showed promising results.[28-30] The major challenges in clinical translation surround the isolation and purification of such a rare population of cells. Therefore, efforts to expand and activate Treg have great biological and clinical relevance. We have previously demonstrated that a single injection of αDR3 to donor animals resulted in significant expansion of Treg, and transplantation using unmanipulated T cells from animals treated with αDR3 had dramatically reduced risk of inducing GVHD.[11] In this report, we further explored the effect of αDR3 signaling on Treg phenotype, gene expression profile, and function and also evaluated the effect of the timing of αDR3 treatment on GVHD risk.

viSNE analysis allows mapping of multicolor flow cytometry or mass cytometry data into 2-dimensional data without changing the high-dimensional structure of the data.[15] Indeed, 45 different 2-dimentional panels of the DR3-Treg phenotype were converted into 10 viSNE maps in total (Figure 1B; supplemental Figure 1). We previously demonstrated that DR3 activation in donor mice expanded central memory $Foxp3^+$ Treg without affecting other T-cell populations. Our current viSNE data clearly showed that several activation or maturation molecules, such as ICOS, Lag3, CD103, and KLRG1, but not CD25, were upregulated in DR3-Treg (Figure 1; supplemental Figure 1). In comprehensive gene expression analysis, the data also suggested that Treg expanded through DR3 activation showed an activated phenotype compared with isotype control Ab-treated Treg (Figure 2). The DR3-Treg expressed several chemokine and activation molecules at higher levels than Iso-Treg. In contrast, anti-apoptotic molecules such as *Bcl2* were downregulated, and apoptotic molecules, such as *Casp1* and *Casp4*, were upregulated. Considering the upregulation of KLRG1 and CD103, which are maturation molecules for Treg,[22] longer therapeutic effects of DR3-Treg might be limited. Indeed, GVHD in DR3-Treg-injected mice began to progress around day 40 to 60 after transplant (Figure 4D), although DR3-Treg-treated animals had better overall survival (Figure 4E). In murine GVHD models treated with freshly isolated Treg, the suppression of donor T-cell activation at early points after transplantation is critical.[31] These early effects of the DR3-Treg may explain the improved survival benefit in these mice, even though the Treg showed a fully mature phenotype (Figure 4E).

The role of TL1a-DR3 signaling in conventional T cells has previously been explored.[5,12,32] In several autoimmune disease models, TL1a-DR3 signaling plays an important role in local T-cell-dependent inflammation through promotion of proinflammatory cytokine secretion after TCR stimulation. These data imply that αDR3 treatment of recipient mice could promote GVHD-related inflammation. In this study, we explored the timing of αDR3 treatment to the recipient mice either before or after allogeneic HCT, with dramatically different results. Transplanted mice treated with αDR3 after alloantigen exposure showed significant allogeneic donor T-cell proliferation and worsened GVHD lethality (Figure 5). These data suggested that the use of αDR3 for GVHD treatment might enhance T-cell activation and accelerate disease. In contrast, αDR3 treatment when used for prophylactic purposes resulted in enhanced survival (Figure 6). In this setting, expansion of recipient-derived Treg and the suppression of donor T-cell proliferation were observed, resulting in the reduction in GVHD severity and lethality. Treg are thought to be more resistant to irradiation than other immune cells.[33] Indeed, our data suggested that residual recipient-derived Treg could expand through DR3 activation and play a role in immune tolerance.

To further explain these disparate results, DR3 expression was found to be significantly increased on $CD4^+Foxp3^-$ T cells after transplantation, whereas DR3 in Treg was downregulated (Figure 5D). These data imply that the $CD4^+Foxp3^-$ T-cell population is more susceptible to αDR3 treatment compared with the residual Treg population. However, the prophylactic treatment with αDR3 administered before alloreactive T-cell stimulation to the recipient mice resulted in improved survival (Figure 6).[11] We and others previously demonstrated that unstimulated recipient-derived Treg were less effective than donor-derived Treg for GVHD treatment.[31,34] However, we and others also recently demonstrated that activation of recipient derived Treg through interleukin 33 or TNFR2 specific agonists could protect from GVHD in murine models.[35,36] These data suggested that the activation/expansion of recipient-derived Treg could be another strategy for preventing GVHD. Here we showed that prophylactic αDR3 treatment preferentially expanded and activated recipient-derived Treg that were critical for GVHD prevention.

Taken together, TL1a-DR3 signaling is a "double-edged sword," where the timing of administration of αDR3 treatment to the recipient mice is critical for regulation of acute GVHD, depending on the activation status of both regulatory and conventional T cells. These results are critically important to understand the biology of this important axis of regulatory and conventional T-cell activation, and also for the potential clinical translation of reagents that may affect DR3 signaling.

In conclusion, we demonstrated that activation through DR3 signaling enhanced the function of Treg; however, this pathway can also further activate alloreactive T cells and has a very different clinical effect, depending on the timing of administration. These data provide important information for future clinical translation using modification of TL1a-DR3 signaling.

Acknowledgments

The authors thank the Veterinary Service Center at Stanford University and the Stanford Shared FACS Facility.

H.N. was supported by Daiichi Sankyo Foundation of Life Science and the Grants-in-Aid for Scientific Research from the Ministry of Education, Culture, Sports, Science and Technology of Japan (15K09493); A.P. was supported by the Fondazione Italiana per la Ricerca sul Cancro; and R.S.N. was supported by the National

Figure 7 (continued) Treg-depleted T cells; $^*P < .05$; $^{**}P < .01$; $^{***}P < .001$; $^{****}P < .0001$). (B) TCD-BM from WT Balb/c mice were transplanted into lethally irradiated B6-Foxp3DTR mice on day 0, and T cells from Balb/c mice were injected on day 2 after transplant. For recipient-derived Treg depletion, DT was injected into recipient mice on days −2, −1, +3, and +5. αDR3 or isotype control Ab was administered to recipient mice on day 0. (i) Experimental scheme. GVHD score (ii) and survival curve (iii) are shown (n = 6 in TCD-BM + D; n = 8 in TCD-BM + T cell + DT; n = 17 in TCD-BM + T cell + D0 αDR3; and n = 12 in TCD-BM + T cell + D0 αDR3 + DT; n.s = not significant; $^{***}P < .001$; $^{****}P < .0001$).

Institutes of Health, National Cancer Institute (P01 CA49605) and National Heart, Lung and Blood Institute (HL075462).

Authorship

Contribution: H.N. and B.-S.K. designed and performed overall experiments, analyzed data, and wrote the manuscript; Y.Y., J.B., A.P., M.A., K.M.-B., M.M., Y.P., and Y.C. performed experiments; Y.Y. and S.C. analyzed and interpreted data and wrote the manuscript; and R.S.N. interpreted the data, provided overall research supervision, and wrote the manuscript.

Conflict-of-interest disclosure: The authors declare no competing financial interests.

ORCID profiles: H.N., 0000-0002-6277-4082.

Correspondence: Robert S. Negrin, Division of Blood and Marrow Transplantation, Department of Medicine, Stanford University, Center for Clinical Sciences Research Building, Room 2205, 269 Campus Dr, Stanford, CA 94305; e-mail: negrs@stanford.edu.

References

1. Croft M, Duan W, Choi H, Eun SY, Madireddi S, Mehta A. TNF superfamily in inflammatory disease: translating basic insights. *Trends Immunol*. 2012;33(3):144-152.
2. Chinnaiyan AM, O'Rourke K, Yu GL, et al. Signal transduction by DR3, a death domain-containing receptor related to TNFR-1 and CD95. *Science*. 1996;274(5289):990-992.
3. Wen L, Zhuang L, Luo X, Wei P. TL1A-induced NF-kappaB activation and c-IAP2 production prevent DR3-mediated apoptosis in TF-1 cells. *J Biol Chem*. 2003;278(40):39251-39258.
4. Gout S, Morin C, Houle F, Huot J. Death receptor-3, a new E-Selectin counter-receptor that confers migration and survival advantages to colon carcinoma cells by triggering p38 and ERK MAPK activation. *Cancer Res*. 2006;66(18):9117-9124.
5. Aiba Y, Nakamura M. The role of TL1A and DR3 in autoimmune and inflammatory diseases. *Mediators Inflamm*. 2013;2013:258164.
6. Sakaguchi S, Yamaguchi T, Nomura T, Ono M. Regulatory T cells and immune tolerance. *Cell*. 2008;133(5):775-787.
7. Wang EC, Thern A, Denzel A, Kitson J, Farrow SN, Owen MJ. DR3 regulates negative selection during thymocyte development. *Mol Cell Biol*. 2001;21(10):3451-3461.
8. Hsieh CS, Lee HM, Lio CW. Selection of regulatory T cells in the thymus. *Nat Rev Immunol*. 2012;12(3):157-167.
9. Taraban VY, Slebioda TJ, Willoughby JE, et al. Sustained TL1A expression modulates effector and regulatory T-cell responses and drives intestinal goblet cell hyperplasia. *Mucosal Immunol*. 2011;4(2):186-196.
10. Schreiber TH, Wolf D, Tsai MS, et al. Therapeutic Treg expansion in mice by TNFRSF25 prevents allergic lung inflammation. *J Clin Invest*. 2010; 120(10):3629-3640.
11. Kim BS, Nishikii H, Baker J, et al. Treatment with agonistic DR3 antibody results in expansion of donor Tregs and reduced graft-versus-host disease. *Blood*. 2015;126(4):546-557.
12. Meylan F, Davidson TS, Kahle E, et al. The TNF-family receptor DR3 is essential for diverse T cell-mediated inflammatory diseases. *Immunity*. 2008; 29(1):79-89.
13. Suffner J, Hochweller K, Kühnle MC, et al. Dendritic cells support homeostatic expansion of Foxp3+ regulatory T cells in Foxp3.LuciDTR mice. *J Immunol*. 2010;184(4):1810-1820.
14. Chen TJ, Kotecha N. Cytobank: providing an analytics platform for community cytometry data analysis and collaboration. *Curr Top Microbiol Immunol*. 2014;377:127-157.
15. Amir el-AD, Davis KL, Tadmor MD, et al. viSNE enables visualization of high dimensional single-cell data and reveals phenotypic heterogeneity of leukemia. *Nat Biotechnol*. 2013;31(6):545-552.
16. Nguyen VH, Zeiser R, Dasilva DL, et al. In vivo dynamics of regulatory T-cell trafficking and survival predict effective strategies to control graft-versus-host disease following allogeneic transplantation. *Blood*. 2007;109(6):2649-2656.
17. Edinger M, Hoffmann P, Ermann J, et al. CD4+ CD25+ regulatory T cells preserve graft-versus-tumor activity while inhibiting graft-versus-host disease after bone marrow transplantation. *Nat Med*. 2003;9(9):1144-1150.
18. Irizarry RA, Hobbs B, Collin F, et al. Exploration, normalization, and summaries of high density oligonucleotide array probe level data. *Biostatistics*. 2003;4(2):249-264.
19. Thornton AM, Korty PE, Tran DQ, et al. Expression of Helios, an Ikaros transcription factor family member, differentiates thymic-derived from peripherally induced Foxp3+ T regulatory cells. *J Immunol*. 2010;184(7): 3433-3441.
20. Weiss JM, Bilate AM, Gobert M, et al. Neuropilin 1 is expressed on thymus-derived natural regulatory T cells, but not mucosa-generated induced Foxp3+ T reg cells. *J Exp Med*. 2012;209(10): 1723-1742.
21. Zhao D, Zhang C, Yi T, et al. In vivo-activated CD103+CD4+ regulatory T cells ameliorate ongoing chronic graft-versus-host disease. *Blood*. 2008;112(5):2129-2138.
22. Cheng G, Yuan X, Tsai MS, Podack ER, Yu A, Malek TR. IL-2 receptor signaling is essential for the development of Klrg1+ terminally differentiated T regulatory cells. *J Immunol*. 2012; 189(4):1780-1791.
23. Feuerer M, Hill JA, Kretschmer K, von Boehmer H, Mathis D, Benoist C. Genomic definition of multiple ex vivo regulatory T cell subphenotypes. *Proc Natl Acad Sci USA*. 2010;107(13): 5919-5924.
24. Schneidawind D, Baker J, Pierini A, et al. Third-party CD4+ invariant natural killer T cells protect from murine GVHD lethality. *Blood*. 2015;125(22): 3491-3500.
25. Taylor PA, Lees CJ, Blazar BR. The infusion of ex vivo activated and expanded CD4(+)CD25(+) immune regulatory cells inhibits graft-versus-host disease lethality. *Blood*. 2002;99(10):3493-3499.
26. Jones SC, Murphy GF, Korngold R. Post-hematopoietic cell transplantation control of graft-versus-host disease by donor CD425 T cells to allow an effective graft-versus-leukemia response. *Biol Blood Marrow Transplant*. 2003; 9(4):243-256.
27. Nguyen VH, Shashidhar S, Chang DS, et al. The impact of regulatory T cells on T-cell immunity following hematopoietic cell transplantation. *Blood*. 2008;111(2):945-953.
28. Martelli MF, Di Ianni M, Ruggeri L, et al. HLA-haploidentical transplantation with regulatory and conventional T-cell adoptive immunotherapy prevents acute leukemia relapse. *Blood*. 2014; 124(4):638-644.
29. Brunstein CG, Miller JS, Cao Q, et al. Infusion of ex vivo expanded T regulatory cells in adults transplanted with umbilical cord blood: safety profile and detection kinetics. *Blood*. 2011;117(3): 1061-1070.
30. Di Ianni M, Falzetti F, Carotti A, et al. Tregs prevent GVHD and promote immune reconstitution in HLA-haploidentical transplantation. *Blood*. 2011;117(14):3921-3928.
31. Pierini A, Colonna L, Alvarez M, et al. Donor requirements for regulatory T Cell suppression of murine graft-versus-host disease. *J Immunol*. 2015;195(1):347-355.
32. Fang L, Adkins B, Deyev V, Podack ER. Essential role of TNF receptor superfamily 25 (TNFRSF25) in the development of allergic lung inflammation. *J Exp Med*. 2008;205(5):1037-1048.
33. Kachikwu EL, Iwamoto KS, Liao YP, et al. Radiation enhances regulatory T cell representation. *Int J Radiat Oncol Biol Phys*. 2011;81(4):1128-1135.
34. Hoffmann P, Ermann J, Edinger M, Fathman CG, Strober S. Donor-type CD4(+)CD25(+) regulatory T cells suppress lethal acute graft-versus-host disease after allogeneic bone marrow transplantation. *J Exp Med*. 2002; 196(3):389-399.
35. Matta BM, Reichenbach DK, Zhang X, et al. Peri-alloHCT IL-33 administration expands recipient T-regulatory cells that protect mice against acute GVHD. *Blood*. 2016;128(3):427-439.
36. Chopra M, Biehl M, Steinfatt T, et al. Exogenous TNFR2 activation protects from acute GvHD via host T reg cell expansion. *J Exp Med*. 2016; 213(9):1881-1900.